

Stability of half quantum vortex in rotating superfluid $^3\text{He-A}$ between parallel plates

T. Kawakami, Y. Tsutsumi, and K. Machida

Department of Physics, Okayama University, Okayama 700-8530, Japan

(Dated: September 21, 2018)

We have found the precise stability region of the half quantum vortex (HQV) for superfluid ^3He A phase confined in parallel plates with a narrow gap under rotation. Standard Ginzburg-Landau free energy, which is well established, is solved to locate the stability region spanned by temperature T and rotation speed (Ω). This Ω - T stability region is wide enough to check it experimentally in available experimental setup. The detailed order parameter structure of HQV characterized by A_1 core is given to facilitate the physical reasons of its stability over other vortices or textures.

PACS numbers: 67.30.he, 67.30.ht, 71.10.Pm

Half quantum vortex (HQV) and associated Majorana zero energy mode have been widely discussed in various research fields in condensed matter physics, ranging from superconductors, superfluids, graphene and fractional Quantum Hall systems[1]. In particular, theoretical and experimental investigations are devoted to finding HQV in superconductors and neutral Fermion superfluids in cold atoms. Recently strong interest on HQV is partly motivated by the fact that the bound state created in the core of HQV is characterized by the Majorana state with the zero energy exactly at the Fermi level. The Majorana particle[2] is thought to be a candidate for quantum computation because it obeys non-Abelian statistics[3] and its existence is protected topologically to avoid decoherence. These situations are ideal for quantum computation[4] if it really exists.

So far there has been no firm experimental evidence for HQV in any superconductors. It is necessary for HQV to exist that superconductivity is described by a chiral p -wave pairing where the \vec{d} vector is able to be free to rotate. It has often been argued that Sr_2RuO_4 may be a prime candidate[5, 6, 7], but strong doubt has been cast on this possibility of Sr_2RuO_4 of its triplet pairing[8, 9, 10]. Note that the first discovered triplet superconductor UPt_3 is an f -wave pairing, not chiral p -wave[11].

Superfluid $^3\text{He-A}$ phase is characterized by a chiral p -wave pairing. There is no doubt on this identification[12]. In fact, Volovik and Mineev[13] are the first to point out the possibility to the realization of HQV in 1976. Since then, there have been several general arguments on the stability of a HQV in connection with $^3\text{He-A}$ phase[14, 15, 16]. However, there are no serious calculations which consider realistic situation in superfluid $^3\text{He-A}$ phase on how to stabilize it and on what boundary conditions are needed for it.

Recently, Yamashita, et al[17] have performed an experiment intended to observe HQV in superfluid $^3\text{He-A}$ in parallel plate geometry. The superfluid is confined in a cylindrical region with the radius $R = 1.5\text{mm}$ and the height $12.5\mu\text{m}$ sandwiched by parallel plates. A magnetic field $H = 26.7\text{mT}(\parallel z)$ is applied perpendicular to the parallel plates under pressure $P=3.05\text{MPa}$. Since

the gap $12.5\mu\text{m}$ between plates is narrow compared to the dipole coherence length $\xi_d \sim 10\mu\text{m}$, the \vec{l} vector is always perpendicular to the plates. Also the \vec{d} vector is confined within the plane because the dipole magnetic field $H_d \sim 2.0\text{mT}$. They investigate to seek out various parameter spaces, such as temperature T , or the rotation speed Ω up to $\Omega = 6.28\text{rad/s}$ by using the rotating cryostat in ISSP, Univ. Tokyo, capable for the maximum rotation speed $\sim 12\text{rad/s}$, but there is no evidence for HQV[17]. Here we are going to give an answer why it is so and to examine the stability region of a HQV which competes with the ordinary singular vortex with the integer winding number and propose a concrete experimental setup which is feasible to perform in the light of the present experimental situation[17].

We start by examining the possible order parameter (OP) forms allowed under the above experimental conditions. The OP of the superfluid ^3He is given by $\hat{\Delta} = i\Sigma_{\mu,i}(A_{\mu,i}\sigma_\mu\hat{p}_i)\sigma_y$ in general where $A_{\mu,i}$ is a 3×3 matrix ($\mu, i = x, y, z$). Among the two known bulk phases as ABM (A) and BW (B) phases, we focus on the A phase in this paper, which is written as $A_{\mu,i} = \Delta_0 d_\mu(\vec{n} + i\vec{m})$ conveniently expressed in terms of the \vec{d} vector and the \vec{l} vector ($\vec{l} = \vec{n} \times \vec{m}$, \vec{n} and \vec{m} are unit vectors forming a triad). The former (latter) vector characterizes the spin (orbital) part of the OP. Since the \vec{l} vector is locked perpendicular to the plates along the z axis and the applied field ($H \parallel z$) perpendicular to the plates confines the \vec{d} vector within the plane (x, y) because it is strong enough compared with the dipole field H_d as mentioned above.

The HQV form originally proposed by Salomaa and Volovik[14], which was followed by others[3, 5, 7], can be expressed as

$$A_{\mu,i} = \Delta_0 e^{i\theta/2} d_\mu(\vec{n} + i\vec{m})_i \quad (1)$$

where $\vec{d} = \hat{x} \cos \frac{\theta}{2} + \hat{y} \sin \frac{\theta}{2}$ (θ is the angle from the \hat{x} axis). Since the \vec{d} vector is assumed to be real here, we call it R-HQV. When winding around the vortex core, the OP exhibits simultaneous change of sign of the \vec{d} vector and shift of the phase θ . Namely, $(\theta, \vec{d}) \implies (\theta + \pi, -\vec{d})$. The

π phase windings of the orbital and the spin parts add up, resulting in 2π phase winding in total. Alternatively, the wave function of this R-HQV form is cast in a form

$$\psi = \Delta_0(r)(e^{i\theta}|\uparrow\uparrow\rangle + |\downarrow\downarrow\rangle)(p_x + ip_y). \quad (2)$$

It is clear that in the R-HQV the $\uparrow\uparrow$ pairs phase-wind by 2π while the $\downarrow\downarrow$ pairs do not. It will turn out shortly that this somewhat restrictive R-HQV form is not a full solution of our Ginzburg-Landau (GL) free energy functional under rotation. Thus we have to seek more general HQV solution to be competitive with the vortex free state stable at rest (A phase texture; AT) and the singular vortex with integer winding (SV). We generalize the OP to find the stable HQV by noticing that the orbital part is doubly degenerate $p \pm ip_y = p_{\pm}$ in addition to doubly degenerate spin space. The most general wave function is spanned by four basis functions, namely,

$$\begin{aligned} \psi = & (A_{++}(r, \theta)|\uparrow\uparrow\rangle + A_{-+}(r, \theta)|\downarrow\downarrow\rangle)p_+ \\ & + (A_{+-}(r, \theta)|\uparrow\uparrow\rangle + A_{--}(r, \theta)|\downarrow\downarrow\rangle)p_- \end{aligned} \quad (3)$$

where each component $A_{\pm\pm}(r, \theta) = A_{\pm\pm}(r)e^{i\theta w_{\pm\pm}}$ can have its own winding number $w_{\pm\pm}$ in the polar coordinates. Under axis-symmetry $w_{++} = w_{--} - 2n$ must be satisfied with $n > 0$ being integer[18]. The winding number combination $(w_{++}, w_{-+}, w_{+-}, w_{--}) = (1, 0, 3, 2)$ is straightforwardly generalized from the above R-HQV form (2), which we are trying to stabilize. The $(0,0,2,2)$ phase is the A phase texture (AT) and $(1,1,3,3)$ is the ordinary singular vortex (SV). The AT is always stable at rest, and HQV and SV compete each other under rotation. Other several phases with different winding number combinations, such as $(0,-1,2,1)$, $(-1,-2,1,0)$ or $(-1,-1,1,1)$ are all irrelevant; namely they are never stabilized. Note that the $(0,-1,2,1)$ phase is stable next to the lowest AT $(0,0,2,2)$ at rest. Under counter clock-wise rotation the chiral $p_+ = p_x + ip_y$ is favored over $p_- = p_x - ip_y$. Thus the $p_+(p_-)$ component constitutes the major (minor) one.

The Ginzburg-Landau (GL) free energy functional is well established[12, 15, 19, 20, 21] and given by a standard form

$$f_{total} = f_{grad} + f_{bulk} + f_{dipole} \quad (4)$$

$$\begin{aligned} f_{grad} = & K[(\partial_i^* A_{\mu j}^*)(\partial_i A_{\mu j}) + (\partial_i^* A_{\mu i}^*)(\partial_j A_{\mu i}) \\ & + (\partial_i^* A_{\mu i}^*)(\partial_j A_{\mu j})] \end{aligned} \quad (5)$$

$$\begin{aligned} f_{bulk} = & -\alpha_{\mu} A_{\mu i}^* A_{\mu i} + \beta_1 A_{\mu i}^* A_{\mu i}^* A_{\nu j} A_{\nu j} \\ & + \beta_2 A_{\mu i}^* A_{\nu j}^* A_{\mu i} A_{\nu j} + \beta_3 A_{\mu i}^* A_{\nu i}^* A_{\mu j} A_{\nu j} \\ & + \beta_4 A_{\mu i}^* A_{\nu j}^* A_{\mu j} A_{\nu i} + \beta_5 A_{\mu i}^* A_{\mu j}^* A_{\nu i} A_{\nu j} \end{aligned} \quad (6)$$

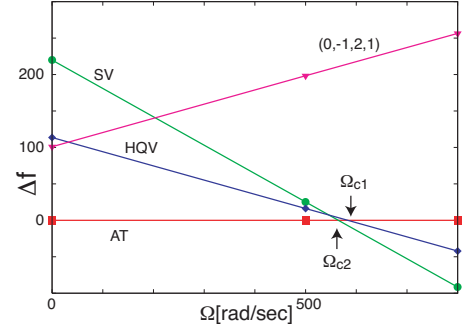


FIG. 1: (Color online) Free energy comparison for AT, HQV, SV and $(0,-1,2,1)$ states as a function of Ω for $R = 10\mu\text{m}$ and $t = T/T_c = 0.95$.

$$f_{dipole} = g_d(A_{\mu\mu}^* A_{\nu\nu} + A_{\mu\nu}^* A_{\nu\mu} - \frac{2}{3}A_{\mu\nu}^* A_{\mu\nu}) \quad (7)$$

where $\partial_i = \nabla_i - i\frac{2m_3}{\hbar}(\vec{\Omega} \times \vec{r})_i$ ($\vec{\Omega}/z$), $\alpha_{\mu} = \alpha_0(1 - T/T_c + \mu\Delta T/T_c)$ ($\mu = \pm$, $\alpha_0 = \frac{N(0)}{3}$), $K = 7\zeta(3)N(0)(\hbar v_F)^2/240(\pi k_B T_c)^2$. g_d is the coupling constant of the dipole interaction, which is $g_d \ll \alpha_0$ [12]. As mentioned above, we assume a two-dimensional system for the OP spatial variation; $\mu, i = x, y$ or \pm . The magnetic field acts not only to pin the \vec{d} vector within the plane, but also to shift the transition temperature T_c by $\Delta t = \Delta T/T_c = (T_{c\downarrow} - T_{c\uparrow})/2T_c$. The fourth order GL coefficients are given by $\beta_1 = -(1 + 0.1\delta)\beta_0$, $\beta_2 = (2 + 0.2\delta)\beta_0$, $\beta_3 = (2 - 0.05\delta)\beta_0$, $\beta_4 = -(2 - 0.055\delta)\beta_0$, and $\beta_5 = -(2 + 0.7\delta)\beta_0$ where $\beta_0 = 7\zeta(3)N(0)/120(\pi k_B T_c)^2$ [15]. The strong coupling correction $\delta > 0$ due to spin fluctuations serves stabilizing the A phase over the B phase in the (P, T) phase diagram[22]. In the following we use the GL parameters[23] tabulated[19, 20, 21] appropriate for the experiment at $P=3.05\text{MPa}$.

We find the free energy minima under the rigid boundary condition $A_{\mu i} = 0$ for $r \geq R$ (R is the radius of the system). A fundamental difficulty associated with the numerical computations lies in the fact that the coherent length $\xi = 10\text{nm}$ is extremely small compared with the system size R where we have to take care of these two length scales in the equal footing in order to accurately evaluate the relative stability among three textures; AT, HQV and SV. This is a reason why this kind of serious energy comparison has not been done before. We carefully calibrate the accuracy of our numerical computation to allow the detailed comparison.

We first consider the weak field case where the transition temperature splitting $\Delta t \simeq 0$. As shown in Fig. 1 we compare three phases with additional other phase mentioned above. It is seen that at rest and lower rotation region AT is stable and eventually upon increasing Ω , SV takes over at Ω_{c2} . Although the HQV is stabler than

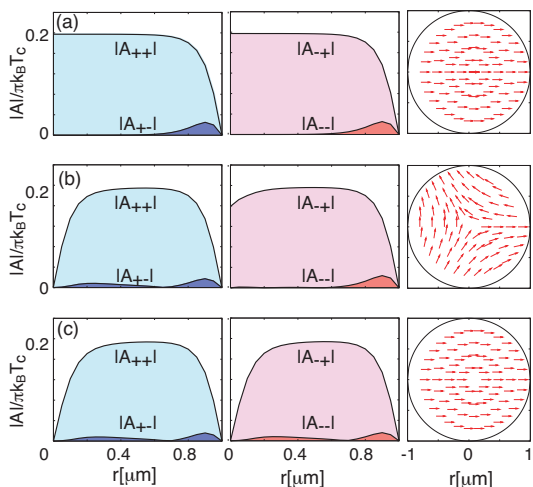


FIG. 2: (Color online) Order parameter and \vec{d} vector profiles for AT (a), HQV (b) and SV (c) for $R = 1.0\mu\text{m}$ and $t = 0.97$. Left and center columns show the cross-section of OP along the radial direction r . Right column shows \vec{d} vector patterns. In (b) it winds by π around the center $r = 0$.

SV at rest situated almost at the half way between AT and SV because the phase winding occurs only for the $\uparrow\uparrow$ pairs. Under rotation the energy gain due to the angular momentum is less than that in SV because of the above reason. Thus HQV is never stabilized under weak field region. We also plot the $(0,-1,2,1)$ state which is second lowest at rest and becomes irrelevant under rotation.

Note that the previous form (2) of R-HQV does not improve this situation, rather becomes worse in its stability. The R-HQV (2) indicates that the vortex core singularity occurs for both $\uparrow\uparrow$ and $\downarrow\downarrow$ pairs even though the latter does not have phase-winding, leading to the additional loss of the condensation energy. The strong coupling effect acts to destabilize both R-HQV and SV relative to AT, thus R-HQV is never stabilized (see below).

In Fig. 2 we illustrate the results of the OP profiles for AT (a), HQV (b) and SV (c) and their \vec{d} vector textures. The OP's in AT are uniform in the central region around $r = 0$, decreasing towards zero at the boundary $r = R$ whose characteristic length is ξ . Thus AT is basically the A phase in the bulk. Near the boundary the induced components A_{+-} and A_{--} appear peripherally.

In HQV (Fig.2(b)) one of the two majority components A_{++} with $w_{++} = 1$ exhibits a phase singularity at $r = 0$, the other component A_{-+} with $w_{-+} = 0$ being depressed slightly there. A_{+-} with $w_{+-} = 3$ and A_{--} with $w_{--} = 2$ are also induced at $r = 0$ and $r = R$. Therefore this HQV profile shows that only the $\downarrow\downarrow$ pairs appears at around $r = 0$, implying the A_1 core state. This tends to stabilize this HQV further compared with R-HQV given by Eq.(2) because (A) the condensation energy loss is less, (B) the fourth order GL energy concerning the interaction term between $\uparrow\uparrow$ and $\downarrow\downarrow$ pairs can

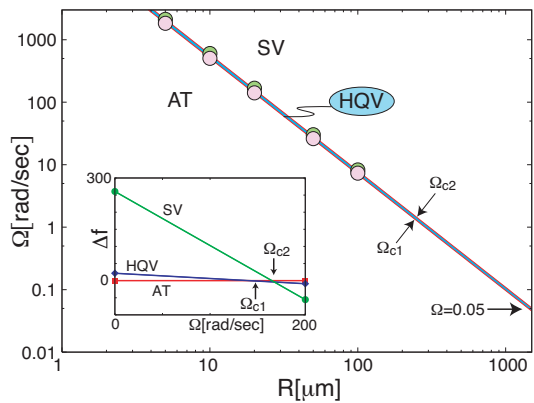


FIG. 3: (Color online) Stability region of HQV sandwiched between Ω_{c1} and Ω_{c2} as a function of R ($t = 0.97$ and $\Delta t = 0.05$). $\Omega_{c1} = 0.05$ rad/sec is the extrapolated value for $R = 1.5\text{mm}$. Inset shows the free energy comparison for $R = 20\mu\text{m}$, displaying the successive transitions from AT to HQV at Ω_{c1} and from HQV to SV at Ω_{c2} .

be expressed as $-4\delta\beta_0|d_+|^2|d_-|^2$. This particular term due to the strong coupling acts to earn the extra gain for this HQV. However, AT is simultaneously stabilized by this term, thus HQV never wins in weak fields. Note in passing that the $\uparrow\uparrow$ and $\downarrow\downarrow$ pairs are completely independent when $\delta = 0$ because the weak coupling GL form is derived under the assumption that the spin space is rotationally invariant. It is seen from Fig.2 that the \vec{d} vector rotates by π when going around the origin in HQV (b) while in the others (a) and (c) it is uniform.

Finally SV in Fig.2(c) exhibits the phase singularities for both major components A_{++} with $w_{++} = 1$ and A_{-+} with $w_{-+} = 1$ and the induced components A_{+-} with $w_{+-} = 3$ and A_{--} with $w_{--} = 3$ appear at the places where the OP spatially varies. Thus this SV is quite advantageous under rotation because they can absorb efficiently the rotational kinetic energy.

Having found that HQV is not stable in weak field region ($H \sim H_d = 10\text{mT}$) both at rest and under rotation, we resort to higher field region; an order of a few kG where $\Delta t \neq 0$ or $T_{c\uparrow} \neq T_{c\downarrow}$. This extension indeed stabilizes the HQV as shown in the inset of Fig. 3 where we compare the three states as a function of Ω . It is seen that as increasing Ω , AT changes into HQV at Ω_{c1} and then HQV to SV at Ω_{c2} . The relative stability region $\Omega_{c1}/\Omega_{c2} \sim 0.8$ which is wide enough to check experimentally.

The reason for the HQV stabilization is physically explained as follows. (A) By introducing Δt which increases (decreases) the OP amplitude of $\downarrow\downarrow$ pair ($\uparrow\uparrow$ pair), the kinetic energy loss due to the phase winding of A_{++} with $w_{++} = 1$, which remains unscreened and spreads out whole system, becomes less compared to AT at rest, meaning that the HQV energy approaches towards the AT energy in Fig. 1 at $\Omega = 0$ as seen from inset of Fig.

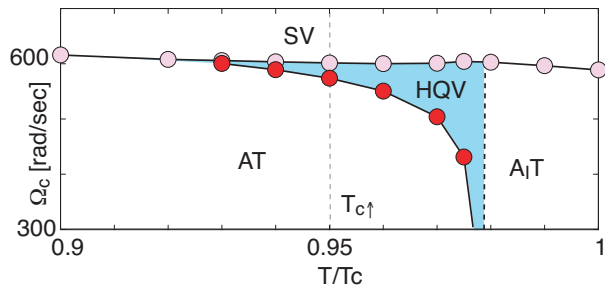


FIG. 4: (Color online) Stability region of HQV in Ω versus T/T_c ($R = 10\mu\text{m}$ and $\Delta t = 0.05$). A_1T denotes the A_1 phase texture where only $\downarrow\downarrow$ pairs exist.

3. Under rotation the HQV energy decreases by absorbing the rotation kinetic energy and eventually becomes lower at Ω_{c1} , which is smaller than Ω_{c2} , stabilizing HQV over SV.

The main panel in Fig. 3 shows Ω_{c1} and Ω_{c2} as a function of the system size R . It is seen that the relative stability region $\Omega_{c1}/\Omega_{c2} \sim 0.8$ stays at a constant against R , keeping 20% region above the critical rotation speed Ω_{c1} at which single HQV is created in the system. The extrapolated Ω_{c1} to $R=1.5\text{mm}$, by which Yamashita, et al[17] have performed experiments, amounts to $\Omega_{c1} \sim 0.05\text{rad/sec}$. The rotation speed stability of the rotation cryostat at ISSP, Univ. Tokyo is accurate enough to perform it. We also notice that by changing the radius R of the system one can control the Ω_{c1} value at will. For example, in $R = 300\mu\text{m}$, $\Omega_{c1} \sim 1\text{rad/sec}$ which is convenient speed to run their rotating cryostat.

In Fig. 4 we depict the temperature dependence of the HQV stability region. We see that the stability region for HQV is widen divergently when approaching the lower critical temperature $T_{c\uparrow}$ from below where the disparity of the OP amplitudes between $\uparrow\uparrow$ pair and $\downarrow\downarrow$ pair increases. Note that the actual lower transition temperature $T_{c\uparrow}$ is shifted slightly upward because the spatially varying $\uparrow\uparrow$ pair OP $A_{-+}(r)$ induces $A_{++}(r)$. In other words, the A_1 phase for $T_{c\downarrow} > T > T_{c\uparrow}$ becomes narrower. Thus one needs not only careful temperature control, an order of 0.01K which is feasible enough, but also theoretical backup to estimate this shift in order to precisely locate the HQV stability region under actual experimental setup.

Since the HQV has the odd winding number for the $\uparrow\uparrow$ pairs, the Majorana quasi-particle with zero energy exactly at the Fermi level, which is localized in the vortex core, is ensured by both the index theorem based on topological argument[24], or directly solving the Bogoliubov-de Gennes equation [25]. These arguments are based on the assumption that the $\uparrow\uparrow$ pair and $\downarrow\downarrow$ pair are completely decoupled. Here the situation is more subtle. The $\uparrow\uparrow$ pair and $\downarrow\downarrow$ pair are interacting through the fourth order GL terms, which is mentioned above. These terms

comes from the strong coupling effect due to ferromagnetic spin fluctuations[22], which ultimately help stabilizing the present HQV. Therefore, it is not obvious completely that the present HQV can accommodate the Majorana fermion with the exactly zero energy. This issue belongs to a future problem.

We also remark on the experimental point that the identification of the HQV is not an easy task. The HQV and SV are indistinguishable by the usual NMR method which utilizes the satellite position in the spectrum[17] because $\vec{d} \perp \vec{l}$ are always kept for both vortices, giving rise to the identical NMR spectra. We suggest small tilting of the field direction from $H \parallel z$ may yield the different NMR signatures. This point deserves further elaboration.

Finally it should be pointed out that our previous theory for the parallel geometry of the superfluid ^3He [25] differs in the field orientation $H \perp z$ there. The singular vortex with odd integer winding number was found in this spinless chiral superfluid. This also gives rise to the Majorana zero energy mode. Thus the field orientations yield different vortices, but those accommodate the Majorana particle localized at each vortex core.

In conclusion, we have found the stability region of half quantum vortex in T - Ω plane of superfluid ^3He A phase confined in parallel plates and given physical reasons why it is stabler than A phase texture or ordinary singular vortex. We propose a concrete experimental setup, which is feasible by using the rotating cryostat such as in ISSP, Univ. Tokyo.

We thank T. Ohmi, O. Ishikawa, M. Yamashita, R. Ishiguro, K. Izumina, M. Kubota, T. Mizushima, M. Ichioka, and G.E. Volovik for useful discussions.

-
- [1] L. Fu and C.L. Kane, Phys. Rev. Lett. **100**, 096407 (2008). P. Ghaemi and F. Wilczek, arXiv: 07092626. J. Nilsson, A.R. Akhmerov and C.W.J. Beenakker, **101**, 120403 (2008). D.L. Bergman and K. Le Hur, arXiv: 0806.0379.
 - [2] “*Ettore Majorana*”, ed. by G.F. Bassani and the Council of the Italian Physical Society (Springer, Heidelberg, 2006).
 - [3] D.A. Ivanov, Phys. Rev. Lett. **86**, 268 (2001).
 - [4] See C. Nayak, et al, Rev. Mod. Phys. (in press).
 - [5] H-Y. Kee, et al, Phys. Rev. B **62**, R9275 (2000), and Europhys.Lett., **80**, 46003 (2007).
 - [6] S. Das Sarma, et al, Phys. Rev. B **73**, 220502(R) (2006).
 - [7] S.B. Chung, et al, Phys. Rev. Lett. **99**, 197002 (2007).
 - [8] K. Machida and M. Ichioka, Phys. Rev. B **77**, 184515 (2008).
 - [9] A. G. Lebed and N. Hayashi, Physica C **341-348**, 1677 (2000)
 - [10] I. Zutic and I. Mazin, Phys. Rev. Lett. **95**, 217004 (2005).
 - [11] K. Machida, et al, J. Phys. Soc. Jpn., **58**, 4116 (1989), and **68**, 3364 (1999). J.A. Sauls, Adv. Phys. **43**, 113 (1994).

- [12] A.J. Leggett, Rev. Mod. Phys. **47**, 331 (1975). D. Vollhardt and P. Wölfle, *The Superfluid phase of Helium 3* (Taylor and Francis, London, 1990).
- [13] G.E. Volovik and V.P. Mineev, JETP Lett. **24**, 561(1976).
- [14] M.C. Cross and W.F. Brinkman, J. Low Temp. Phys., **27**, 683 (1977). M.M. Salomaa and G.E. Volovik, Phys. Rev. Lett. **55**, 1184 (1985).
- [15] M.M. Salomaa and G.E. Volovik, Rev. Mod. Phys. **59**, 3533 (1987).
- [16] G.E. Volovik, *Exotic Properties of Superfluid ^3He* (World Scientific, Singapore, 1992) p.130.
- [17] M. Yamashita, et al, Phys. Rev. Lett. **101**, 025302 (2008).
- [18] T. Isoshima, et al, Phys. Rev. **A60**, 4857 (1999).
- [19] J. A. Sauls and J. W. Serene, Phys. Rev. **B24**, 183 (1981).
- [20] D. S. Greywall, Phys. Rev. **B33**, 7520 (1986).
- [21] T. Kita, Phys. Rev. **B66**, 224515 (2002).
- [22] P.W. Anderson and W.F. Brinkmann, Phys. Rev. Lett. **80**, 1108 (1973).
- [23] The following GL parameters are used: $\alpha_0 = 3.81 \times 10^{50} [J^{-1}m^{-3}]$, and $\beta_1 = -3.75, \beta_2 = 6.65, \beta_3 = 6.56, \beta_4 = 5.99, \beta_5 = -8.53$ in units of $10^{99} [J^{-3}m^{-3}]$.
- [24] S. Tewari, et al, Phys. Rev. Lett. **99**, 037001 (2007).
- [25] Y. Tsutsumi, et al, Phys. Rev. Lett. **101**, 135302 (2008).